A Multidetector Scintillation Camera with 254 Channels

Edda Sveinsdottir, Bo Larsen, Per Rommer, and Niels A. Lassen

University of Copenhagen and Bispebjerg Hospital, Copenhagen, Denmark

A computer-based scintillation camera has been designed for both dynamic and static radionuclide studies. The detecting head has 254 independent sodium iodide crystals, each with a photomultiplier and amplifier. In dynamic measurements simultaneous events can be recorded, and 1 million total counts per second can be accommodated with less than 0.5% loss in any one channel. This corresponds to a calculated deadtime of 5 nsec. The multidetector camera is being used for ^{133}Xe dynamic studies of regional cerebral blood flow in man and for ^{99m}Tc and ^{197}Hg static imaging of the brain.

J Nucl Med 18: 168–174, 1977

The Anger scintillation camera is generally limited to a counting rate of about 30,000 cps, if one is to avoid excessive coincidence loss and the associated deterioration of spatial resolution (*1*). In dynamic brain studies using intra-arterial injection to measure regional cerebral blood flow (rCBF), the maximal counting rate should preferably be about 1,000 cps for each area studied, for otherwise one cannot obtain a reliable washout curve, which usually requires initial time intervals of 1 sec (*2,3*). Therefore, a camera based on an array of individual scintillation detectors, allowing simultaneous processing of events, is a necessity if many regions are to be studied at the same time (*4,5*). The present paper describes such a camera designed primarily for rCBF studies using ^{133}Xe in man. Preliminary descriptions have been presented (*6,7*).

THE MULTIDETECTOR CAMERA

The camera§ contains (A) a transducer head with 254 crystals, each with a photomultiplier and an amplifier, and (B) an electronic section that functions as an interface to the computer (Fig. 1). These two components are physically separate so that the transducer head may be moved.

Transducer head. The transducer head is constructed so that its anterior surface is a thick concave aluminum plate forming part of a spherical surface with its center 20 cm in front of the surface. Into this aluminum plate the 254 sodium iodide crystals are fitted in a matrix with 19 columns and

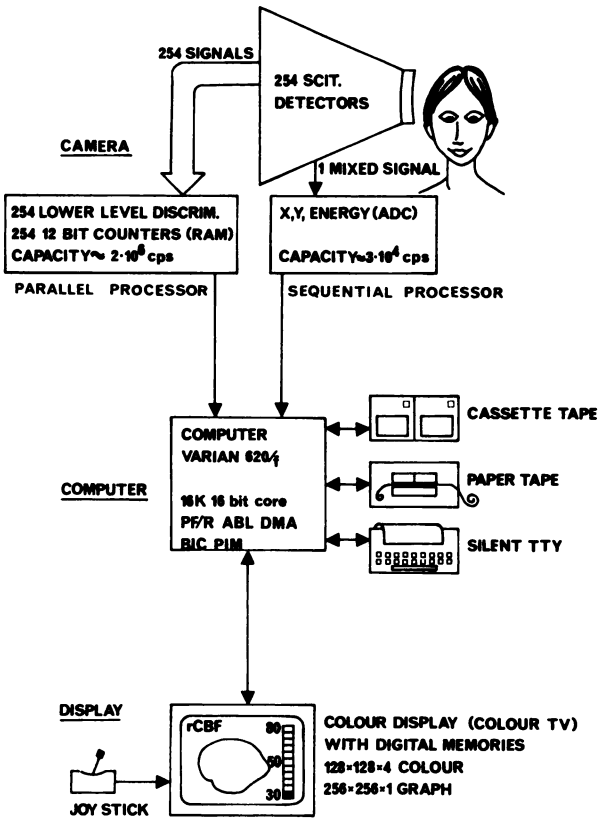

FIG. 1. Block diagram of multidetector camera.

Received Nov. 20, 1975; revision accepted Aug. 19, 1976.

For reprints contact: N. A. Lassen, Dept. of Clinical Physiology, Bispebjerg Hospital, DK-2400 Copenhagen NV, Denmark.

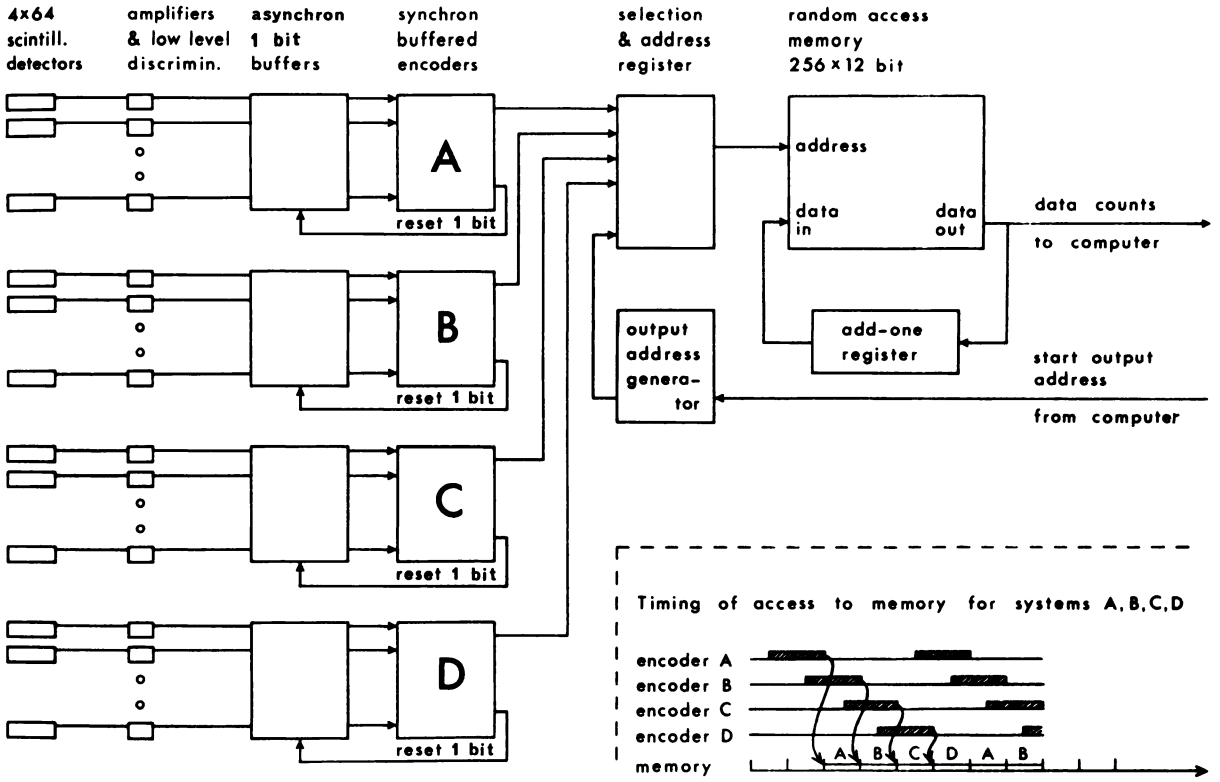

FIG. 2. Schema for parallel-event processor. After threshold selection, pulses from 254 detectors are registered in 254 one-bit asynchronous buffers. Instead of using polling scheme to store counts in 254-word memory, asynchronous buffers are read into 254 one-bit synchronous buffers at time intervals of 1,280 nsec. Address is then encoded in fixed priority sequence for each group of 64 detectors, memory word belonging to selected detector is incremented by 1, and its asynchronous buffer bit reset. Since encoding time is longer than memory cycle time (320 nsec), four 64-detector groups timeshare memory.

14 rows (three elements omitted in each corner), the rows and columns being 1 cm apart. The crystals are cylindrical, 0.8 cm in diameter, and 1.0 cm long.

A Plexiglas light guide, 25 cm long and 0.9 cm in diameter, connects each crystal to its individual photomultiplier, the latter having an outer diameter of 2 cm. The photomultipliers are connected to amplifiers with a 1-μsec differentiation step and a simple lower-level discriminator set for approximately 25 keV. The gain of each amplifier can be adjusted by potentiometer.

Collimation. Two collimators are available: they are 4-cm-thick lead slabs, concave in shape in order to fit the front surface of the detector. The holes, one for each crystal, are cylindrical. In one collimator the holes are 7 mm in diameter and are parallel, making the detector "look" straight ahead in spite of the collimator's concavity. The other collimator has 8-mm converging holes; these give an enlargement factor of $\sim$1.5 at the surface of the brain.

Electronics. The electronic part of the camera has two independent sections, one for parallel and one for sequential processing of events. The *parallel-event processor* (Fig. 2) functions as a 254-channel multicounter. After lower-level discrimination, the pulses are added up in a small digital memory that can be read by the computer according to a timetable set by the computer program. Each counter can store 4,095 events before overflow occurs. By using both asynchronous and synchronous 1-bit buffers for each detector (arranged in four blocks of 64) and letting the four blocks timeshare access to the memory (cycle time, 320 nsec), a very high overall count-rate capacity is obtained.

The sequential-event processor (Fig. 3) includes an 80-nsec 6-bit analog-to-digital converter (ADC) for the measurement of the voltage of each individual pulse above the threshold level. This coarse 64-level pulse-height analysis is considered adequate because the energy resolution of the individual scintillation detectors is poor: the FWHM at 80 keV is about 30 keV. Information about the energy and the position (detector number) of each event is held in a four-stage first-in–first-out buffer that acts as a derandomizing device until transfer to the computer can take place, thus ensuring no loss of events due to the deadtime of the computer (*1*).

Thus, the essential difference between the two processors is that the parallel processor permits registration of simultaneous events, retains no pulse-height information, and permits a very high count rate, whereas the sequential processor handles one

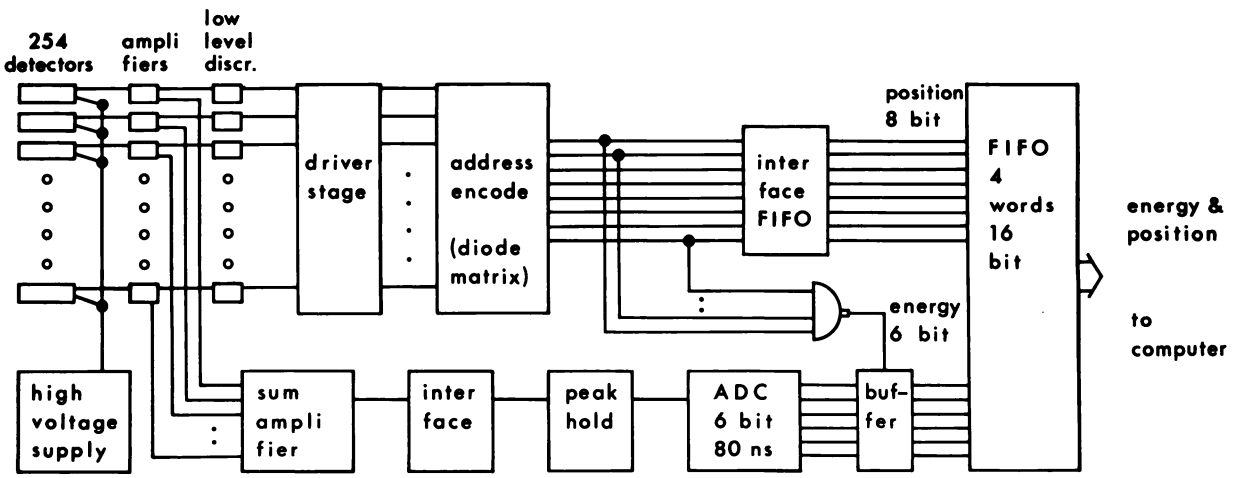

FIG. 3. Schema for sequential-event processor. After threshold pulse-height selection, incoming photon's position is encoded (8 bits for detector number). At same time pulse height is measured and converted to 6-bit binary word. Position and energy information for event is then stored in 4-word first-in–first-out buffer until it is transferred to computer.

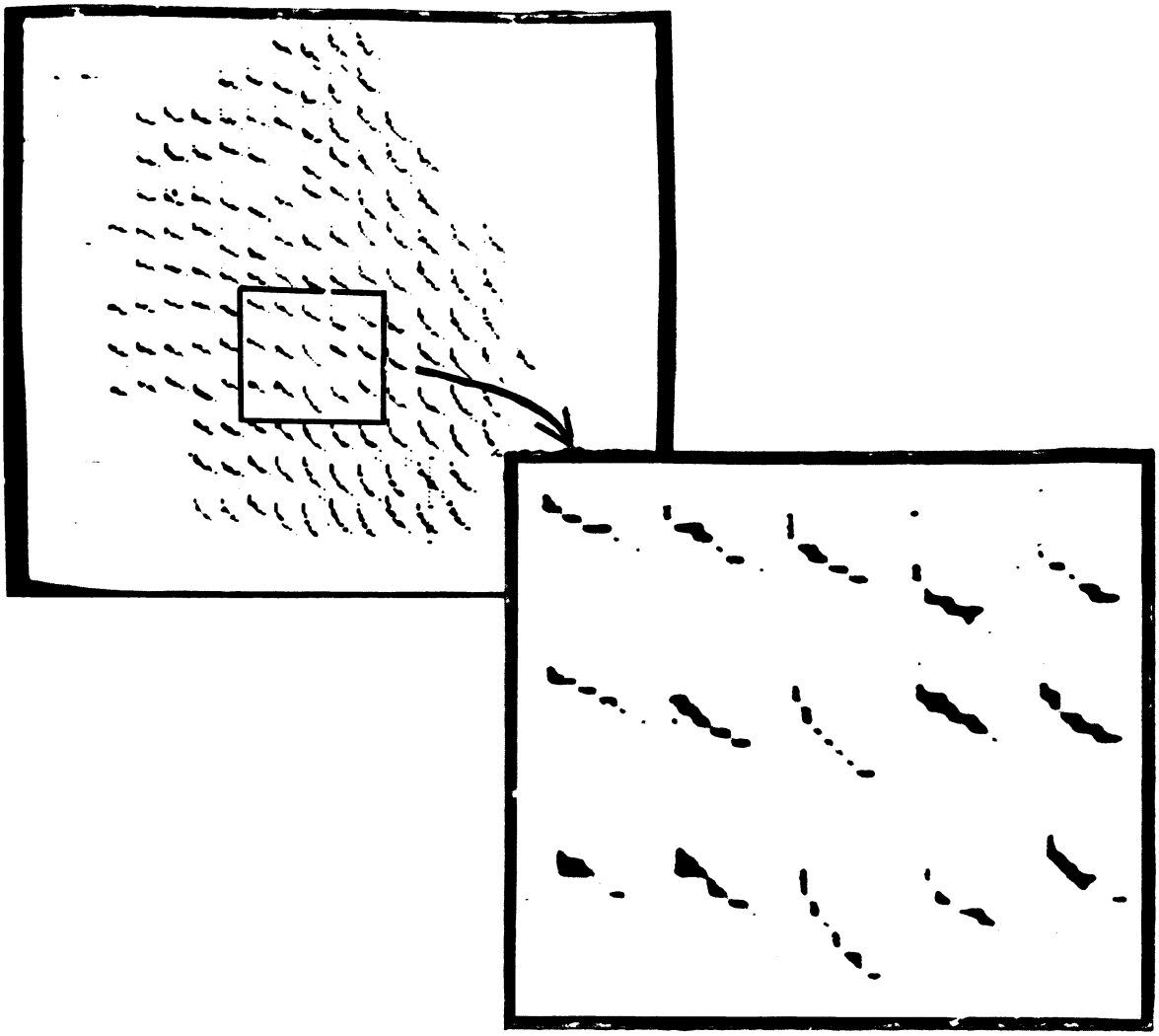

FIG. 4. Spatial resolution of dynamic rCBF studies. In case of epilepsy, steepness of two curves, surrounded by much gentler slopes, is shown in blow-up. Steep curves represent fast rCBF of about 100 ml/100 gm-min in diseased area and are seen to continue into very large area of steep curves below and to right in original picture. Less steep curves correspond to flow about 50 ml/100 gm-min. Highly significant differences in steepness (factor of 2) can be seen in adjacent channels and hence, in principle, an abnormally high regional blood flow may become manifest in one channel alone.

event at a time but with a correspondingly lower count rate. The pulses are fed to the same ADC, preserving the pulse-height information. The pulse-height discrimination is performed in software individually for each detector.

THE COMPUTER SYSTEM

Computer configuration. The computer* has a 16K core memory storing 16-bit words (cycle time, 750 nsec) and is equipped with a paper-tape system and a fast typewriter console. There is no backup storage in the form of disk or drum, but cassette tape or floppy disks are planned for patient data and program systems. A display system† using a color TV monitor is connected to the computer. The system has two semiconductor memories: a color memory displaying on the TV screen as a 128 × 128 raster of areas that can be colored in 16 levels, and a black-and-white memory with 256 × 256 resolution for displaying texts and graphs.

Two program systems have been developed: a general image-handling program system (IMAGE) and a special-purpose system (CBF). All programs are written in ASSEMBLER code.

Image system. In the IMAGE system emphasis has been placed on the interactive use of the camera. To make a study fully automatic, sequences of functions to be performed can be prespecified: for example, data acquisition, background subtraction and sensitivity correction, scaling, interpolation, and display. Physiologic trigger signals can be used to activate a function interactively, permitting, for example, on-line ECG-gated cinecardiography with cumulative data sampling over many heart beats. Data acquisition can take place using the parallel- or the sequential-event processor or both. To keep the camera tuned, a set of calibration functions is included, the most important being a spectral analysis program to collect energy spectra for all the detectors and perform automatic window setting. This eliminates the need for manual gain adjustment of the detectors, except in cases of severe drift. The image-processing functions include image arithmetic, rotation, interpolation, and definition of areas of interest. A more extensive description of the IMAGE system has been reported (*7*).

CBF system. The data (counts in each detector) are accumulated in fixed time intervals according to a timetable, using 1-sec intervals initially with longer intervals later. Each data frame is displayed on the TV monitor so that the arrival and washout of the ^{133}Xe bolus are followed visually throughout the study. After 2 min the curves are displayed in semilogarithmic scale on the TV monitor, using the graph memory, allowing visual inspection of all raw data (Fig. 4). At the same time the calculated values for initial rCBF slope are displayed as a functional image in fixed color scale, affording a preliminary on-line overview of the results (*8*). The rapid availability of the results allows the planning of conditions for a subsequent ^{133}Xe injection 15 or 20 min later, e.g., with altered blood pressure or CO_2 tension, or with the patient performing some voluntary motor task.

The CBF system is being extended to a biexponential analysis using the slope-height-area-moment (SHAM) type of rapid analysis (*9*).‡ However, the biexponential model is not appropriate in many disease states (*10*).

PERFORMANCE

Spatial resolution. The resolution was evaluated using a line-source of ^{133}Xe. With the parallel collimator (7-mm holes), the FWHM was 0.9 cm at a constant 3 cm from the collimator face and with a human skull between source and detector to imitate in vivo scatter. With the source aligned over one row of holes, the count rates for the two adjacent rows were 10% of the central value. This indicates a FWHM of 0.9 cm, as is shown by integration of a typical line spread function (*11*). With the converging collimator (8-mm holes), also at 3 cm, where it magnifies about 1.5 times, the resolution is practically the same.

With this resolution it should be possible to obtain significant information from one channel only. This has been verified, since ^{99m}Tc-pyrophosphate uptake

FIG. 5. Case of tumor studied using ^{197}Hg scintigraphic imaging. Left hemisphere, nose to left. Converging collimator is used in lower picture to verify increased uptake indicating extension of tumor in posterior direction seen using parallel collimator. Each image has undergone background subtraction, correction for nonuniformity, and interpolation.

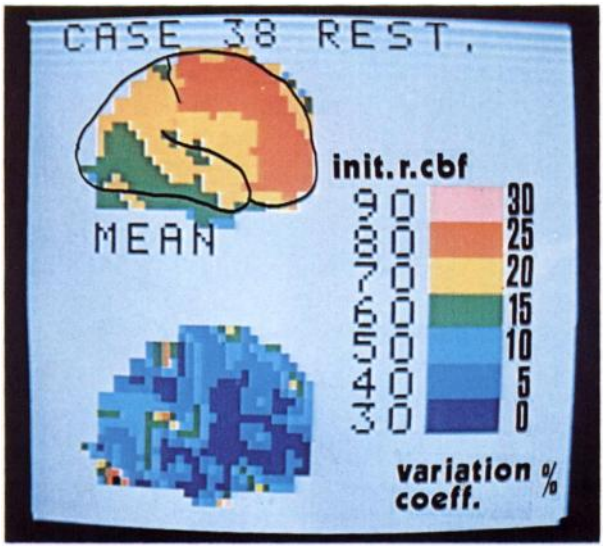

FIG. 6. Map of regional cerebral blood flow in a normal subject and coefficient of variation based on three consecutive rCBF studies made at intervals of 20 min.

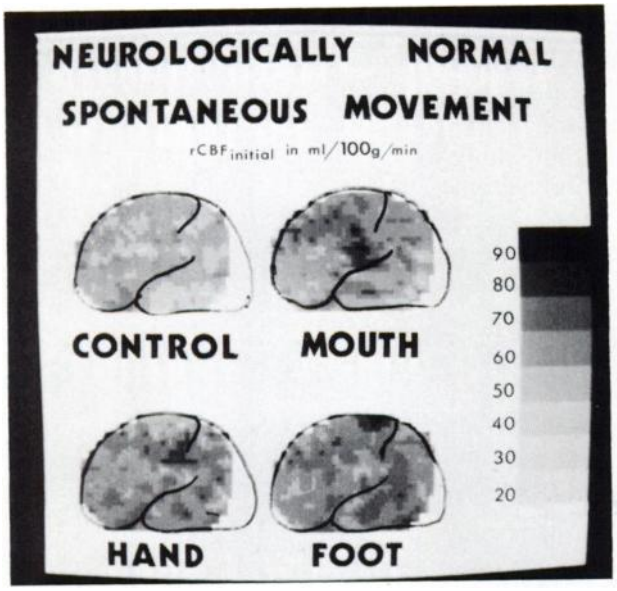

FIG. 7. Activation of three different parts of brain by voluntary movement of opposite foot, hand, and part of mouth. Regions of increased rCBF correspond to known anatomic areas in primary sensorimotor cortex (18).

has been observed on several occasions in one channel alone in static bone scans of metastatic cancer of the vertebral column, the finding being verified by conventional x-rays. In the case of rCBF studies using ^{133}Xe, the same type of observation has been made (Fig. 4).

Temporal resolution. In the parallel-event processing mode, the calculated deadtime of the multidetector camera was found to be 5 nsec for the instrument as a whole at count rates up to 10^6 cps. This corresponds to a pulse loss of 0.5% at 10^6 cps, a loss that is evenly distributed over the matrix and that does not influence the spatial resolution. In our clinical rCBF studies (8–10 mCi of ^{133}Xe), the maximum count rate is around 3×10^5 cps; hence, no deadtime correction is needed.

In the sequential-event processing mode the maximum tolerable count rate is determined by the pulse-width of the events and is the same as in other sequential-event processing cameras, namely, about 30,000 cps. The computer handling of the events, including routine energy discrimination and histogram-mode acquisition, poses an upper limit on the acceptable event rate. For standard data acquisition this limit is 50,000 cps, and for acquisition performing on-line spectral analysis it is 35,000 cps.

Clinical results. During 2 years of operation we have made more than 700 static brain images with ^{99m}Tc and ^{197}Hg (Fig. 5). Invariably we use prior exposure to a uniform source to provide correction for uneven channel response.

The dynamic rCBF studies with ^{133}Xe (more than 100 to date) are checked by arteriographic studies. The normal initial rCBF is 50–70 ml of blood per 100 gm of brain per minute, the highest values being found anteriorly (Fig. 6). Such studies, in triplicate, yield a coefficient of variation of around 5% for rCBF in the main part of the injected side (Fig. 6). We can observe regional hyperemia following re-

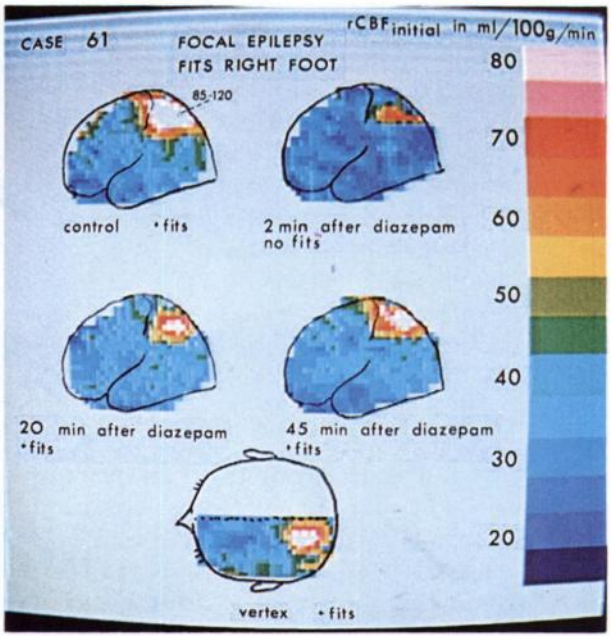

FIG. 8. Case of cortical epilepsy with marked focal hyperemia. Immediately after 2-mg injection of diazepam, seizure in contralateral foot stopped, and hyperemic region diminished in extent and intensity. Electroencephalogram was completely normal during this part of study.

gional voluntary movement, and the involved cortical areas follow the expected neurologic pattern (Fig. 7). Studies with visual perception and speech have shown other activation patterns. Thus, the cerebral centers for various functions can be located.

Data are accumulating on patients with brain disease. In acute vascular occlusion we often find an abnormal rCBF even when the carotid angiogram is essentially normal. In 10 cases of focal cortical epilepsy (*12*), an increased rCBF pointed out the epileptogenic area (Fig. 8) better than did the EEG, which was sometimes entirely normal.

CONCLUDING REMARKS

A multidetector scintillation camera has been designed primarily for studies of the brain or similar-sized organs. The camera has proven versatile, since it permits the generation of routine scintigrams as well as measurement of cerebral blood flow, displaying the regional distribution of the flow as a functional image.

Detailed comparison with other scintillation cameras is postponed, but it is clear that only the multicrystal system of Bender and Blau could approach our multidetector camera in temporal resolution. Yet, as applied to rCBF studies with ^{133}Xe, the deadtime of the multicrystal scintillation camera system was 22 μsec for the instrument as a whole (*13*). Our experience with the prototype leads us to emphasize particularly the *digital* nature of the system. The pulses are recorded in individual scintillation counters, thus giving the positional information, just as in the retina of the human eye. In the past this approach has been avoided in routine scintillation cameras because of the cost of the detectors. We have simplified and miniaturized the associated electronics and have let the computer handle traditional hardware tasks such as energy discrimination and camera calibration. In this way the cost of the prototype has been kept about the same as for a conventional single-crystal camera equipped with comparable computer capabilities. Nevertheless, the cost of 254 photomultipliers is significant. It would be better if a smaller device (solid state) could be used to detect the scintillations in the crystals.

The variation of sensitivity with target depth is another problem. In cerebral studies the sampled tissue mass consists of a truncated cone of many layers, with about 20% of the events being Compton scatter from elsewhere in the brain (*13*). This constitutes a serious hazard, because areas of ischemia can coexist with areas with normal or above-normal flow within the same tissue cone. Hence, the camera is almost blind to small ischemic areas and totally blind to nonperfused areas that are "looked through" simply because no tracer is carried into that area (*14*). K. Guldberg points out (personal communication) that there exists a possibility, still unexploited, that the mass of tissue seen by a detector could be estimated from the area of the washout curve, after appropriate correction for the detector's sensitivity function and its normal distribution. However, even such calculations would not tell us where, within the truncated cone, the area of zero flow is located. A truly three-dimensional method for studying radionuclide distribution is afforded by computerized axial tomography as developed by Kuhl et al. (*15,16*). Some potential may exist for performing dynamic rCBF studies using positron-emitting tracers and coincidence detection (*17*), but quite severe problems will have to be overcome to get the image-sampling time down to around 1 sec, as is required by the dynamic studies we are doing. These comments on three-dimensional imaging serve to emphasize the two main limitations of the two-dimensional rCBF images obtained with the multidetector camera: (A) the rCBF images underestimate low blood flow, especially if normal or above-normal flow coexists in the same detector field; and (B) the rCBF images would be quite markedly influenced by extracerebral ^{133}Xe if the gas were supplied atraumatically by inhalation instead of by intracarotid injection. A successful technique should minimize both limitations.

ACKNOWLEDGMENTS

We wish to thank K. Andersen for discussions and ideas on the parallel-event processor, P. Torlöf for design of the computer interface, M. Tuschman for work on the sequential-event processor, and T. Schomacker, K. Schubell, and J. Bang for their assistance with the programming.

FOOTNOTES

§ Medimatic, Ltd., Copenhagen, Denmark.

* Varian 620/f computer (Walnut Creek, Calif.).

† Atomenergi A/B, Studsvik, Sweden.

‡ In Ref. *14* an error in the sign of the quantity S has been made. The correct final equations are

$$(MH - A^2)\alpha_2^2 + (HA - SM)\alpha_2 + (SA - H^2) = 0,$$
$$(M_TH - A_TA)\alpha_2^2 + [H_T(HT - 2A_T) + HA_T - SM_T]\alpha_2 + [H_T(2H - H_T - ST) + SA_T - H^2] = 0.$$

REFERENCES

1. Cox JR, Hill RL, Mullani NA: Interface design considerations. In *Computer Processing of Dynamic Images from an Anger Scintillation Camera*, Larson KB, Cox JR, eds. New York, Society of Nuclear Medicine, 1974, pp 33–51

2. Høedt-Rasmussen K, Sveinsdottir E, Lassen NA: Regional cerebral blood flow in man determined by intra-arterial injection of radioactive inert gas. *Circ Res* 18: 237–247, 1966

3. Kanno I, Uemura K: Some experimental errors in calculating regional cerebral blood flow from the intracarotid ^{133}Xe clearance curve. *Stroke* 6: 370–375, 1975

4. Fucks W, Knipping HW, Liese E, et al.: Zur diagnostischen Verwendung von Isotopen am Krankenbett, ins

besondere in der Hertz und Krebsklinik. *Atomkernenergie* 9: 271–278, 1964

5. SVEINSDOTTIR E, LASSEN NA, RISBERG J, et al.: Regional cerebral blood flow measured by multiple probes: An oscilloscope and a digital computer system for rapid data processing. In *Cerebral Blood Flow*, Brock M, et al. eds. Berlin, Springer Verlag, 1969, pp 27–29

6. SVEINSDOTTIR E, LASSEN NA: A 256 detector system for measuring regional cerebral blood flow. *Stroke* 4: 365, 1973

7. SVEINSDOTTIR E, SCHOMACKER T, LASSEN NA: Interactive handling of regional cerebral blood flow data using a macrolanguage. In *Proceedings of the IVth International Conference on Information Processing in Scintigraphy, Orsay, 1975*, Raynaud C, Todd-Pokropek A, eds. Orsay, France, Commissariat á l'Energie Atomique, 1975, pp 209–220

8. OLESEN J, PAULSON OB, LASSEN NA: Regional cerebral blood flow in man determined by the initial slope of the clearance of intra-arterially injected ^{133}Xe. *Stroke* 2: 519–540, 1971

9. CAPRANI O, SVEINSDOTTIR E, LASSEN NA: SHAM, a method for biexponential curve resolution using initial slope, height, area and moment of the experimental decay type curve. *J Theor Biol* 52: 299–315, 1975

10. PALVÖLGYI R: Regional cerebral blood flow in patients with intracranial tumors. *J Neurosurg* 31: 149–163, 1969

11. WAGNER HN, ed.: *Principles of Nuclear Medicine*. Philadelphia, W. B. Saunders, 1969

12. HOUGAARD K, OIKAWA T, SVEINSDOTTIR E, et al.: Regional cerebral blood flow in focal cortical epilepsy. *Arch Neurol* 33: 527–535, 1976

13. CANNON PJ, SCIACCA RR, BRUST JCM, et al.: Measurement of regional cerebral blood flow with ^{133}Xe and a multiple-crystal camera. *Stroke* 5: 371–383, 1974

14. DONLEY RF, SUNDT TM, ANDERSON RE, et al.: Blood flow measurements and the "look through" artifact in focal cerebral ischemia. *Stroke* 6: 121–131, 1975

15. KUHL DE, EDWARDS RQ: Image separation isotope scanning. *Radiology* 80: 653–662, 1963

16. KUHL DE, EDWARDS RQ: Reorganizing data from transverse section scans using digital processing. *Radiology* 91: 975–983, 1968

17. HOFFMAN EJ, PHELPS ME, MULLANI NA, et al.: Design and performance characteristics of a whole-body positron transaxial tomograph. *J Nucl Med* 17: 493–502, 1976

18. ROLAND PE, LARSEN B: Focal increase of cerebral blood flow during stereognostic testing in man. *Arch Neurol* 33: 551–558, 1976